Available online at www.sciencedirect.com
SCIENCE DIRECT®
Coordination Chemistry Reviews 250 (2006) 155–169
COORDINATION CHEMISTRY REVIEWS
www.elsevier.com/locate/ccr

Review

Site selective ligand modification and tactic variation in polypropylene chains produced with metallocene catalysts

Abbas Razavi [a,*], Ulf Thewalt [b]

[a] *Centre de Recherche Du Groupe Total, Zone Industrielle C, B-7181 Seneffe (Feluy), Belgium*
[b] *Sektion für Röntgen und Elektronen Beugung Univeristät Ulm, Belgium*

Contents

1. Introduction 155
2. Results and discussion 156
   2.1. C_s symmetry, enantiotopic sites, and chain migratory insertion mechanism 156
   2.2. Frontal substituents and their impact on stereoselectivity 159
   2.3. Chain migratory insertion versus chiral site epimerization; counter-ion effect 160
3. Distal substituent, site transformation, C_1 symmetry 161
   3.1. Chain "stationary" insertion mechanism 161
   3.2. Proximal substituent and combined proximal/distal substituent effect 162
   3.3. Perfect chain stationary insertion, perfect isoselectivity 163
4. A more dynamic model 164
5. C_1 symmetry versus symmetry C_2 166
6. Experimental 166
   6.1. Synthetic part 166
   6.2. X-ray data 166
   References 168

Abstract

This review covers the stereochemistry of propylene insertion/propagation reactions with a variety of C_s and C_1 symmetric, bridged cyclopentadienyl-fluorenyl ligands containing metallocene catalysts for the preparation of highly stereo-regular polypropylene. The article discusses the syndioselectivity of metallocenes with local C_s symmetry and two enantio-topic coordination positions, and proof that from all the different possible substitutional positions, only those performed in the frontal positions of the fluorenyl ligand are effective in improving the syndio-selectivity of the final catalysts. It further establishes that the bilateral symmetry selection rule is not a sufficient condition and will be "ignored" by the system, whenever symmetric "excess" in steric bulk is present. An unsymmetrical "excess" in steric forces, induced by a bulky distal substituent on the other hand, will provoke a full tactic inversion as a consequence of an irreversible C_s/C_1 site transformation. The review also covers the combined distal, proximal, and frontal substituent effect and their impact on molecular weight and regio- and stereoregularity of the final polymers. Finally, isoselective C_2 and C_1 symmetric systems are compared with respect to their potential for commercial application.

Keywords: Metallocene catalysts; Olefin polymerization; Polypropylene; Syndiospecificity

1. Introduction

The contribution of metallocene single site catalyst research, besides enlarging the diversity space of the exist-

* Corresponding author. Tel.: +32 64 514072.
E-mail address: abbas.razavi@total.com (A. Razavi).

0010-8545/$ – see front matter © 2005 Published by Elsevier B.V.
doi:10.1016/j.ccr.2005.07.006

ing polyolefin libraries, is due to their inherent molecular nature which enables precise analytical characterization and more insight about the pre-catalysts' structures, active sites transition states, and corresponding polymer microstructures. Additionally, their narrow disperse polymers also can be much easier subject to accurate physical measurements and rheological tests. The improved identification of the sites in turn allows, through a well established, in most cases direct site symmetry/polymer-stereochemistry relationship, us to inflict systematic structural alterations, in a quasi-iterative fashion, to arrive at preconceived polymer(s) with designed architectural thus physico-mechanical characteristics. The stereochemistry of propylene polymerization with a C_s symmetric bridged cyclopentadienyl-fluorenyl containing ligand has been thoroughly investigated since its discovery by us in the late 1980s [1a–f]. They have contributed much to our basic understanding of olefin coordination polymerization. Current, generally accepted transition state structural models for metallocene catalysts' active sites, are derived from single crystal X-ray diffraction data of the catalyst precursor or its stabilized metallocenium-alky cation.

Despite its static nature, the model satisfactorily delineates the origin of the observed micro-structural particularities of the principal sequences and the presence of different types of stereo defects in isotactic, syndiotactic and stereo block type polypropylene chains. Recent new structural discoveries, experimental observations, and theoretical considerations, however, are suggestive of a more dynamic model with flexible and changing geometries, before, during, and after the coordination/insertion processes [2].

Our recent observations have also shown that for isospecific system, the C_2 symmetry and helical chirality limitation can be lifted. Current high performance C_1 symmetric catalyst systems with central site chirality can be similarly or better isotactically selective. In this contribution, we review the central dogmas of both *iso*-and syndiotactic specificity with a given class of metallocene catalysts with a bridged cyclopentadienyl-fluorenyl ligand skeleton and describe the impact of the substitutional modification in each case starting with C_s symmetric systems.

2. Results and discussion

2.1. C_s symmetry, enantiotopic sites, and chain migratory insertion mechanism

The X-ray determined molecular structures of (η5-C_5H_4─CMe_2-η5-$C_{13}H_8$)MCl_2; M = Zr(1), Hf(2) [1f] that were used to prepare the first highly crystalline syndiotactic polypropylene samples are presented in Fig. 1.

The structure, catalytic properties, and the origin of the formation of syndiotactic chains with . . . r r r r r r r r m r r r r r r r r r m m rr r r r r r . . . microtacticity have already been discussed exhaustively in numerous publications [1,3,4,5a,6a and b], however, for the sake of continuity in the line of evidence, the highlights of these discussions will be reiterated below:

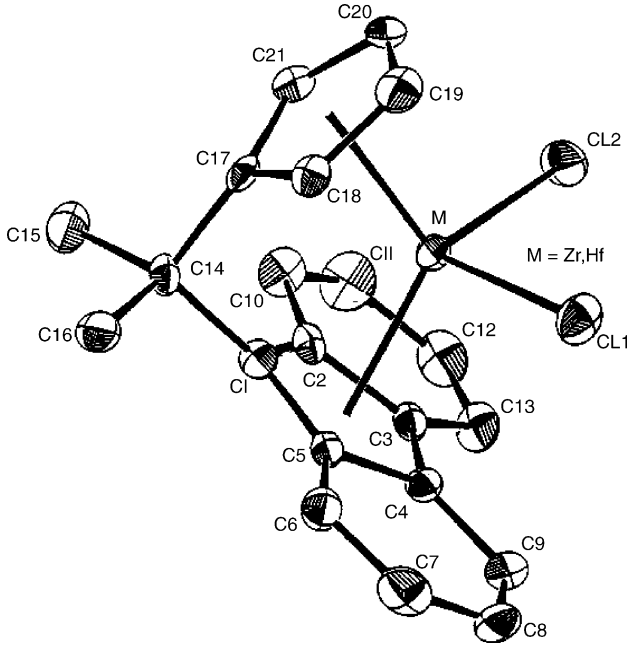

Fig. 1. X-ray determined molecular structure of (η5-C_5H_4─CMe_2-η5-$C_{13}H_8$)MCl_2; M = Zr, Hf.

[The . . . r r r r r r r . . . symbols are indicative of sequences of ramic dyads (two propylene units with opposite relative configurations is designated as racemo, r). A perfect syndiotactic chain should contain long sequences of these r dyads. The m and mm are occasional stereo-errors of two or three monomers with the same relative configuration and are called meso-dyads and meso-triads. From these stereo errors we can deduce the mechanism of polymerization.]

(1) Stereorigid metallocene procatalyst is prochiral and possesses bilateral symmetry (Fig. 1).
(2) The chiral, cationic alkyl metallocenium species [1h] which are formed after the activation are composed of equal numbers of *R* and *S* enantiomers and have the necessary vacant position and fragment orbitals for the coordination and activation of incoming propylene monomers (Fig. 2).
(3) The *R* and *S* enantiomers are monomer π-face selective. The re- and si face selectivity, is ligand assisted and is induced by the unique steric arrangement of the chelating organic ligand engulfing the resident transition metal center. Via a delicately balanced, cooperative, and non-bonded steric interaction contributed by different parts of the "living" catalytic species—the ligand, directs the polymer chain's chiral orientation which in turn defines the monomer's coordinating mode (Fig. 3). The non-bonded steric interactions govern the whole scenery of syndiospecific polymerization processes, coordination, insertion, propagation and termination.

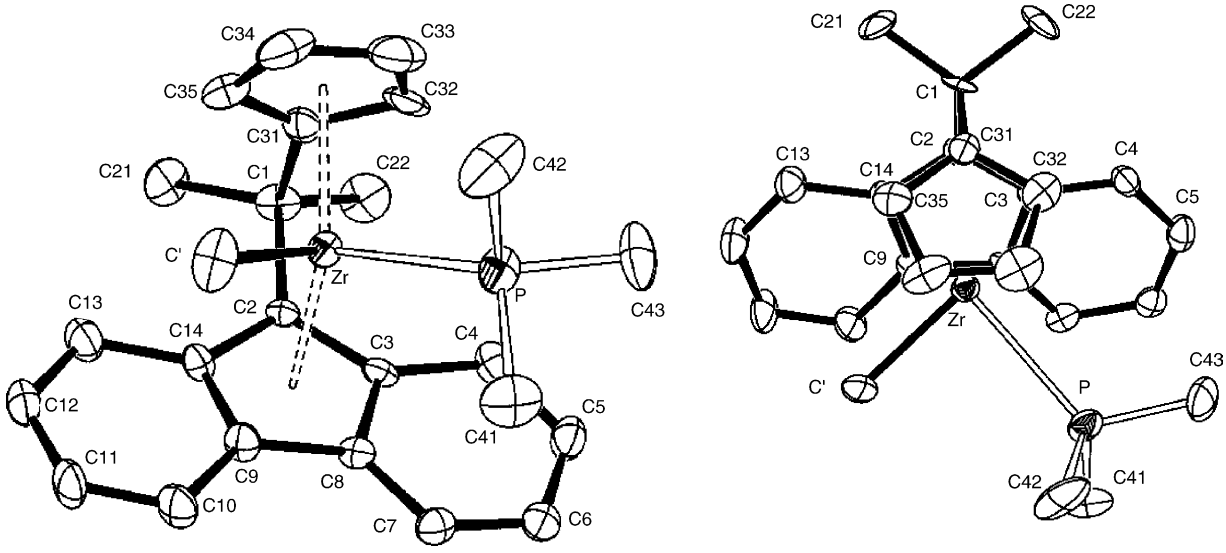

Fig. 2. Two views of the cation in the salt $[(\eta^5\text{-}C_5H_4{-}CMe_2\text{-}\eta^5\text{-}C_{13}H_8)ZrMe(PMe_3)]^+[B(C_6F_5)_4]^-$. On the right, the $[(\eta^5\text{-}C_5H_4{-}CMe_2\text{-}\eta^5\text{-}C_{13}H_8)ZrMe]^+$ cation is stabilized here with trimethylphosphine which occupies the monomer coordination position [1h].

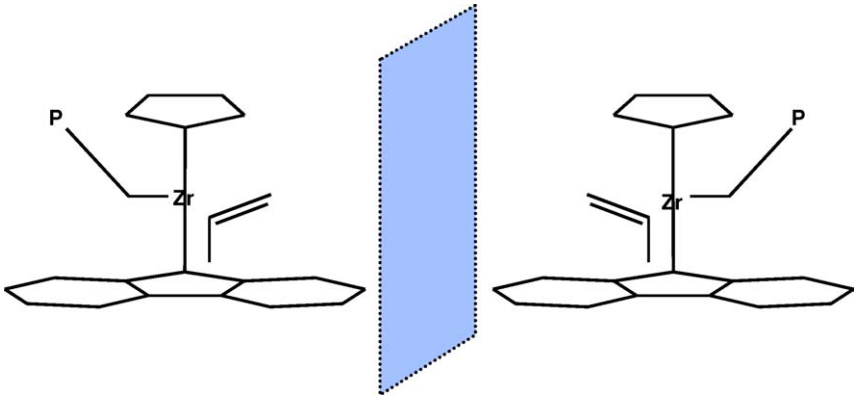

Fig. 3. Transition state structure (left) and possible monomer coordination mode with the enantiomorphous active species (right).

(4) According to these assumptions each enantiomer, independently, would produce isotactic chains yet an exclusively syndiotactic polymer is formed. Thus, we conclude that the active species interconvert in a systematic way after each monomer insertion (Scheme 1). The systematic transformation of the two antipodes into one another implies that the relative positions of at least two of the four ligands surrounding the transition

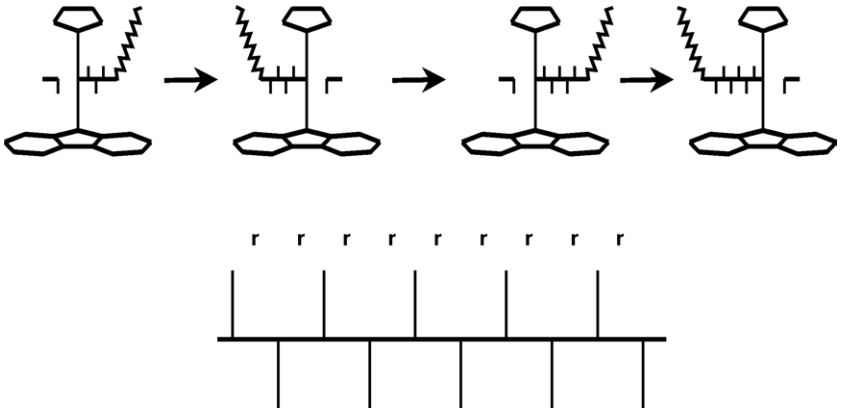

Scheme 1. Mechanism of syndiospecific polymerization (top). Fischer projection of a perfect syndiotactic chain.

metal are exchanged continuously. Since the η^5 bonded aromatic ligands are tied together by a structural bridge and their rearrangement is not possible, such an interconversion can only take place when the alkyl group (polymer chain) and the coordinating monomers exchange their positions systematically (chain migratory insertion!).

(5) The meso triad enantiomorphic site stereochemical control related errors, mm, are formed whenever the said balanced non-bonded steric interaction is perturbed. In such a case, a monomer with "wrong face" will be inserted and a unit with inverted configuration is enchained (mm defects). The ability for reverse face selectivity emanates from inherent static structural factors and is independent of monomer concentration.

(6) The origin of the monomer concentration and temperature dependent m type stereo-errors is more complex and more difficult to discern. Their formation is explained according to the site epimerization mechanism (vide infra).

This model has been proposed based on relative importance of the non-bonded steric interactions between different parts of the aromatic ligand, the growing polymer chain, and the coordinating monomer in the following manner. The steric interaction between the flat and spatially extended fluorenyl ligand forces the growing polymer chain to adopt a conformation which orients itself towards the free space left (or right) of the unsubstituted cyclopentadienyl moiety of the ligand. The incoming monomer in turn – to avoid excessive steric exposure – orients itself in a manner to have its methyl group *trans* (or anti) positioned with respect to the growing polymer chain. In this coordinated mode, the monomer points with its methyl group head down into the empty space in the central region of the fluorenyl ligand (Fig. 3). The steric interaction between the flat and spatially extended fluorenyl ligand, forces the growing polymer chain to be oriented towards the free space left (or right) to the unsubstituted cyclopentadienyl moiety of the ligand. The incoming monomer – to avoid excessive steric exposure – orients itself in a manner to have its methyl group in a *trans* position with respect to the growing polymer chain. In this orientation, the coordinated monomer points with its methyl group head down into the empty space in the central region of the fluorenyl ligand (Fig. 3).

The "head down" coordination mode of the monomer was determined after extensive molecular mechanics and force field calculations performed by Corradini, Cavallo and coworkers [7]. The model underwent later additional refinement and took its current form after experiments conducted by several groups [8] established an α C–H agostic bond assistance in the transition state. One of the many merits of the syndiotactic specific system was that it provided, for the first time, solid proof for the cationic nature of the active site and chain migratory mode of insertion that had been hypothesized decades ago.

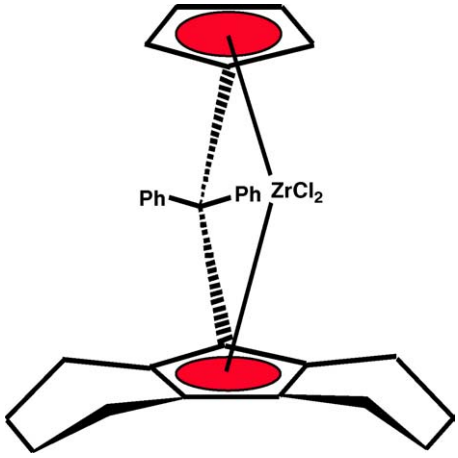

Fig. 4. Molecular structure of (η5-C_5H_4–CPh_2-η5-$C_{13}H_{16}$)$ZrCl_2$ (**3**).

It is apparent that the syndiospecificity as discussed above is the result of the combined and simultaneous actions of several factors; the absence or excess of each could lead to malfunctioning of the catalyst and destruction of the syndioselectivity process. The presence of the delicate steric balance between all the active site's participants as well as proper functioning of the dynamic processes involved (chain migration, site epimerization ion-pairing, etc.) is essential for its existence. To elaborate this point we shall discuss the catalytic properties of metallocene (η5-C_5H_4–CPh_2-η5-$C_{13}H_{16}$)$ZrCl_2$ (**3**) [1j] for propylene polymerization (Fig. 4). Complex **3** is formed by hydrogenation of the highly syndiotactic specific precursor, (η5-C_5H_4–CPh_2-η5-$C_{13}H_8$)$ZrCl_2$ [1g]. Molecule **3**, like its precursor, possesses all the structural and symmetry requirements one would impose on a would-be syndiospecific system, yet after activation it produces perfectly atactic polypropylene chains.

Obviously, the bilateral symmetry of the metallocene precatalyst could not have ensured, in this case, the syndioselectivity of the final catalyst. The excess symmetric steric interaction exerted from crucial distal parts of the octahydro-fluorenyl moiety of the ligand eliminates the potential syndiotactic specific properties of a perfectly C_s symmetric catalyst system. The minor change, from benzenic CH groups to slightly larger cyclohexenylic CH_2 groups in the fluorenyl distal positions, has perturbed the balance of steric forces and annihilated the syndioselection process completely. The substituent change (CH to CH_2) is concomitant, in this particular case, with the dynamic phenomenon, of boat/chair like conformation interconversion. The pseudo-axial/equatorial C–H geometry change in the flexible cyclohexenylic parts of the octa-hydrogenated fluorenyl increases the dynamic volume of the CH_2 group and may be the real reason behind syndio-selectivity loss. The example of **3** and other similar C_s symmetric aspecific systems [9], reveals the delicacy of the concerted actions of steric and dynamic forces and the difficulties to be encountered while improving the syndioselectivity in general.

One way to increase the stereoregularity of the syndiotactic polypropylene, is to lower the site epimerization rate by polymerizing at very high monomer concentration (e.g. in liquid propylene) and/or by polymerizing at the lowest possible temperatures. It is of practical interest, however, to reach this goal by structural modifications and/or by playing with the counter ion composition and interaction. The structure/counter-ion modification approach, if successful, should lower both the percentage of single m containing rmrr pentads and decrease the concentration of the rmmr pentads by enhancing the inherent enantioselectivity of the active site via improved steric balance. From the many substitutional changes that have been performed on the original bridged cyclopentadienyl-fluorenyl MCl_2 structures and the available data, the following statements can safely be made:

(1) Additional substitution on the cyclopentadienyl part of the ligand is irrelevant (proximal) or detrimental (distal) to the syndioselectivity of the final catalyst [10].
(2) Modifications of the substituents in the bridge section will have little or no effect on the stereoselectivity of the catalysts, however, these are crucial for the molecular weights of the resulting syndiotactic polymers [1g].
(3) Substitution modifications in the fluorenyl moiety will have little or no detrimental impact on the stereoselectivity of the final catalyst, except when the substitution is performed in frontal position(s) such 3, 6 or both [3].

2.2. *Frontal substituents and their impact on stereoselectivity*

To demonstrate the substituent effect in these positions we shall discuss the polymerization properties of metallocene (η5-C_5H_4–CPh_2-η5-3,6-di-^{t}But-$C_{13}H_6$)$ZrCl_2$ (**4**) [3b–e] whose molecular structure is given in Fig. 5. When activated, **4** very efficiently polymerizes propylene to highly syndiotactic polypropylene; showing almost three times higher activity than **1**. Table 1 presents the results of polymerization and analyses of the syndiotactic polymers produced with the **4**/MAO catalyst system at different polymerization temperatures [3b–e]. Table 2 compares the corresponding rmrr and rmmr pentad concentrations of syndiotactic polymers produced with **1** and **4**. A cursory look at the data given in Tables 1 and 2 reveals that substitution in positions 3 and 6 causes substantial improvement in stereoselectivity of the final catalysts by decreasing both meso dyad and triad related stereo errors. The rmrr pentad concentrations in polymers produced with **4** are lower than observed for polymers of **1**; they double in size for both systems with every 20 °C increase in polymerization temperature. On the other hand, the rmmr pentad concentrations in polymers of **4** are about half in size with respect to the corresponding pentad concentrations determined for polymers of **1** and much less temperature dependent.

Table 1
Polymerization results and polymer analyses for **4**/MAO catalysts system

T (°C)	M_w (D)	rrrr (%)	Regiodefects (%)	Mpt. (°C)
40	766,000	91.0	nd	150
60	509,000	88.5	nd	143
80	443,000	79.0	nd	128

D, Dalton; nd, not detected.

Table 2
Stereodefects generated in the polymers produced with **4**/MAO (left) and **1**/MAO (right)

T (°C)	**4**/MAO		**1**/MAO	
	rmmr (%)	rmrr (%)	rmmr (%)	rmrr (%)
40	0.73	0.93	1.55	1.15
60	0.85	1.99	1.65	2.70
80	1.06	3.79	2.20	4.82

The improved stereoselectivity, (lower rmmr %) for **4** could be explained by the two-fold beneficial presence of bulky *t*-butyl substituents at positions 3 and 6, in directing the polymer chain to the most preferred upward conformation left or right to the cyclopentadienyl group, and by providing a more effective guidance for the head down monomer coor-

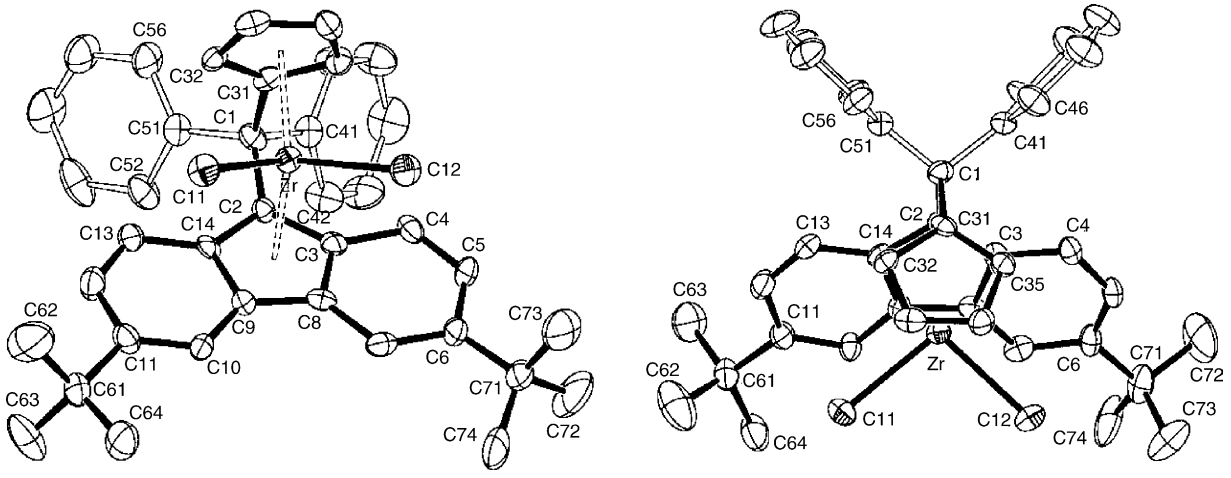

Fig. 5. Two views of the molecular structure of (η^5-C_5H_4–CPh_2-η^5-3,6-di-^{t}But-$C_{13}H_6$)$ZrCl_2$ (**4**).

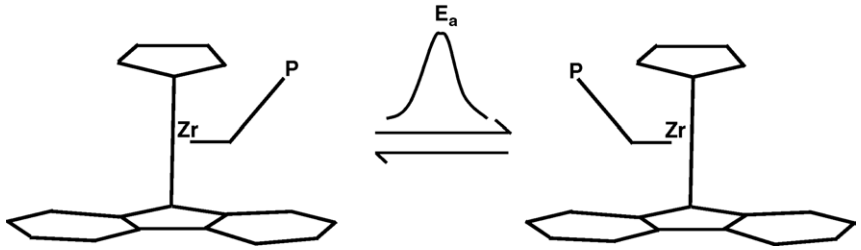

Fig. 6. Schematic presentation of endothermic active site epimerization process.

dination mode (more efficient stereoselectivity by creation of smaller "chiral pocket"). The explanation for lower rmrr pentad concentration in polymers produced with **4** versus **1**, at the same polymerization temperature and monomer concentration, is however, less straight forward. It might be related to the steric bulk of the *tert*-butyl groups rendering the site epimerization more difficult or different cation/anion association/dissociation dynamics [11]. Fig. 5 presents two different views of the molecular structure of (η5-C_5H_4–CPh_2-η5-3,6-di-^{t}But-$C_{13}H_6$)$ZrCl_2$ (**4**), determined by single crystal X-ray diffraction methods. A cursory glance at the top and front views of **4** suggests that any potential contact ion pairing with MAO anion would be different and harder for **4** than for **1** due to the substantial steric bulk of the *tert*-butyl substituents. In the latter case, the anion could approach the metallocenium cation without any obstacle and with ease. Thus, the preventive effect of the *tert*-butyl substituents on contact ion pairing in **4** may well be an additional factor for improved stereoselectivity of **4**/MAO as a result of slower active site epimerization rate. In this context, it should be noted that the contact ion-paring effect on site epimerization is different and separate from polar solvent effect. In the latter case, the polar solvent molecules coordinate and successfully compete with monomer molecules for the available coordination site, leading to an increase of site epimerization and a lowering of stereoregularity of the polymers produced with syndiotactic specific catalyst systems.

2.3. Chain migratory insertion versus chiral site epimerization; counter-ion effect

The concept of site epimerization can be explained according to the scheme shown in Fig. 6 and is in principle very close to the mechanism of chain back migration proposed by Cossee and Arlman [12]. According to these authors, the polymer chains connected to active $TiCl_5R$ sites, imbedded in the ionic lattice, undergo systematic back migration after each insertion due to the changes in the relative ionicity of their immediate environments. In the case of metallocene catalysts, the close proximity of a polar molecule, the counter ion, and the intermittent or permanent blockage of one of the two coordination sites via a tight contact ion-pairing or bulky substituent could be the driving force and/or enhancing factor for the site epimerization involved processes.

By favoring the less crowded, "lipophilic" site, the polymer chain systematically moves away from the polar and crowded environment of the opposite coordination position and migrates back after each insertion. We had suspected and suggested [1f] this mechanism to be the cause for the formation of short isotactic blocks detected in the backbone of the predominantly syndiotactic polymer chains formed with **2**. Fig. 7 present the methyl region of the ^{13}C NMR spectra of syndiotactic polymers produced with **1** and **2**. The Hf related spectrum indicates

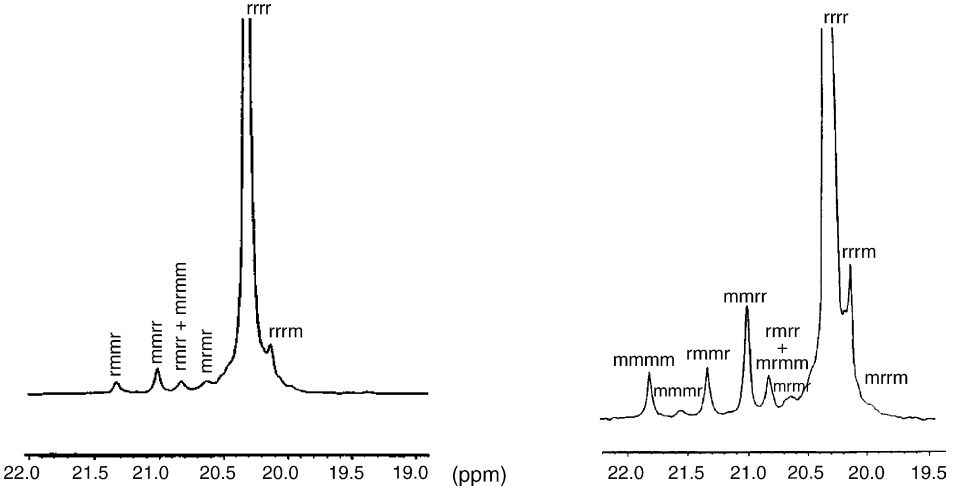

Fig. 7. ^{13}C NMR spectrum of syndiotactic polypropylene produced with Zr (left) and Hf (right) based catalysts.

the presence of about 2% of mmmm pentads (peak at 21.85 ppm), which could have been formed as a result of tighter ion pairing between the MAO anion and Hf cation [1f].

Under these conditions, the contact ion-paired complex active site, with temporary coordination site in-equivalency, undergoes a reversible C_s/pseudo-C_1 site symmetry transformation. Several insertions at the same enantiomorphic coordination site may occur to form a short isotactic sequence within the predominantly syndiotactic chain. The lower activity of the catalysts and higher molecular weights of the polymers formed with the **2**/MAO catalyst system could also be related to this tight contact ion-pairing. The close proximity of the anion partially "quenches" the electrophilicity of the Hf-cation, lowers the Hf–C bond polarization, and decreases the propagation rate by increasing the insertion activation energy barrier. Low Lewis acidity of the cation, on the other hand, lowers its propensity for β-hydride abstraction, and leads to an increase in the molecular weight of the polymers. The observation made by Rieger [11b] that the "non-coordinating" anion bearing activators, such as trityltetrakis(pentafluorophenyl)borate provide substantially higher activities for hafnocene-based catalysts is certainly in agreement with this argument.

The coordination site inequivalency caused by occasional contact ion pairing can be become permanent by introduction of a large enough distal substituent. The substituent's repulsive steric interaction with the migrating polymer chain will enhance the site epimerization. The epimerization rate increases to dominate the insertion rate, and with it the frequency and length of the isotactic sequences in the predominantly syndiotactic chains [4]. Comparing several different substituents implanted in the distal position of **1**, the most remarkable results were obtained with a *tert*-butyl group as the bulky substituent [5]. In this case, the process of site epimerization is manipulated to the extent that the tactic behavior of the catalyst was completely reversed and an originally syndiospecific catalyst, by adding a "simple" substituent, produced "purely" isotactic polymer chains.

Table 3
Results of polymerization and the polymer analyses for the **5**/MAO catalyst system

T (°C)	M_w (kDa)	mmmm (%)	Regiodefects (%)	Mpt. (°C)
40	75,000	78.02	0.4	129
60	62,000	77.47	0.4	127
80	48,000	75.80	0.4	127

3. Distal substituent, site transformation, C_1 symmetry

3.1. Chain "stationary" insertion mechanism

The formation of the isotactic polymers with the aforementioned catalyst with the tertiary butyl group was explained according to a mechanism that we described as chain "stationary" insertion. According to this mechanism, from the perspective of the incoming monomer, the growing polymer chain appears "stationary" by attacking predominantly from the same coordination position [5,6b]. As shown in Fig. 8, the role of the *tert*-butyl group is instrumental in creating the condition for coordination site differentiation by breaking the symmetry and causing permanent a C_s/C_1 site transformation. The crystal structure and polymerization behavior of the (η5-3-^{t}But-C_5H_4–CMe_2-η5-$C_{13}H_8$)$ZrCl_2$ (**5**) have been discussed elsewhere [5].

Table 3 summarizes the polymerization results and some polymer properties obtained with **5**/MAO. The absence of rmrm and mrmr [6a and b] pentads indicating the very low probability of occurrence of two consecutive stereo-errors, reflects the low probability for the chain to reside at the more crowded coordination position and provides the key clue for the accelerated site epimerization processes in this catalyst system. Additionally, the polymerization temperature insensitivity (or enhancing) [6a,c and d] of the isospecificty of **5**/MAO (vide infra)—in drastic contrast to Brinzinger type C_2 symmetric isoselective systems [13] can be seen as a further clue for the operating epimerization processes. Finally, molecular mechanic analysis and energy calculations performed by Guerra et al. on similar systems are also supportive

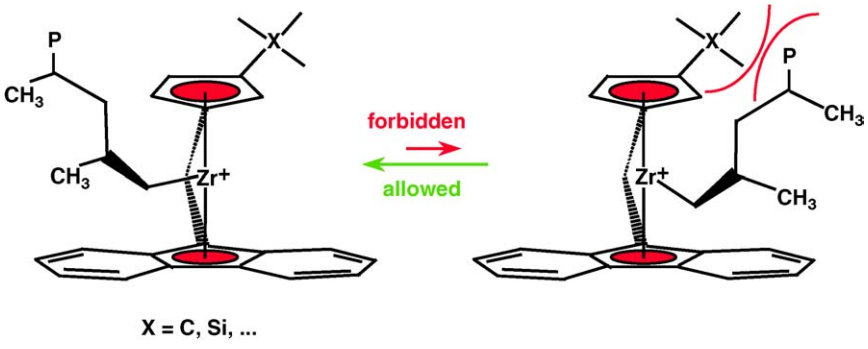

Fig. 8. Repulsive steric repulsion between the polymer chain and β-substituent provoking the accelerated site epimerization.

Table 4
Results of polymerization and the polymer analyses with the **6**/MAO system

T (°C)	M_w (kDa)	mmmm (%)	Regiodefects (%)	Mpt. (°C)
40	580,000	79.12	nd	132
60	402,000	86.3	nd	144
80	213,000	83.6	nd	142

nd, Not detected.

of a site epimerization controlled mechanism for this catalyst [6e and f].

3.2. Proximal substituent and combined proximal/distal substituent effect

A critical look at the data in Table 3 reveals that despite the very interesting academic aspects of this catalyst system, the resulting low molecular weight isotactic polymers are of little practical interest. The polymer stereo regularities are relatively low and the chains are plagued with non-negligible amounts of regiodefects. To improve and to understand better the catalytic behavior of **5** we decided to modify its structure with a second, smaller substituent in the proximal position and prepared metallocene molecules, (η5-3-^{t}But-5-Me-C_5H_2–CMe_2-η5-$C_{13}H_8$)$ZrCl_2$ (**6**) [14]. The MAO activated complex **6** is a very effective catalyst for isospecific polymerization of propylene. Table 4 present the results of polymerization and analyses of polymers produced in liquid propylene at different temperatures with the **6**/MAO catalyst system.

Close inspection of the data given in Table 4 indicates that the introduction of the *trans*-proximal methyl substituent in this molecule has brought about substantial improvements in almost every aspect of the catalytic performance. The molecular weights of the polymers produced with **6** are substantially higher than those reported for **5** and isotactic chains are practically devoid of regiodefects. Most importantly, the stereo regularities (mmmm%) of the polymer chains produced with **6** are, substantially higher, by about 10%, than the stereo regularities registered for polymers produced with catalyst **5**/MAO.

As a consequence, the melting points of the corresponding isotactic polymers reach values over 140 °C even for the polymers formed at 80 °C. Noteworthy is the increase of stereoregularity with increasing polymerization temperature from 40 to 60 °C and its subsequence slight decrease by increasing the polymerization temperature to 80 °C. An apparent drastic suppression of β-hydride elimination and 2-1 insertion related processes must have led to a substantial increase in molecular weights, and regio- and overall stereoregularity of the polymers. Fig. 9 presents two perspective views of molecular structure of **6** determined by single crystal X-ray diffraction analysis. These views illustrate pictorially the position of the proximal methyl group (designated by C41), in the back section of the molecule. It is positioned in such way that it would necessarily interfere with the methyl group of the propylene monomer in a 2-1 coordinated mode (should the monomer choose this coordination position). In this position, it also interferes sterically with a cyclic transition state structure – prerequisite for any kind of β-hydride transfer – involving the transition metal, polymer chain and monomer.

Whereas the rationalization of the β-hydride elimination suppression seems straight forward, and is in line with observations that have been made for bridged substituted bicyclopentadienyl and bisindenyl based metallocene catalyst systems [13], the mechanism of the suppression of 2-1 insertion needs further discussion.

Considering the fact that for C_1 symmetric systems (the type discussed here) the probability of monomer coordination/insertion at the less crowded site is very low, the

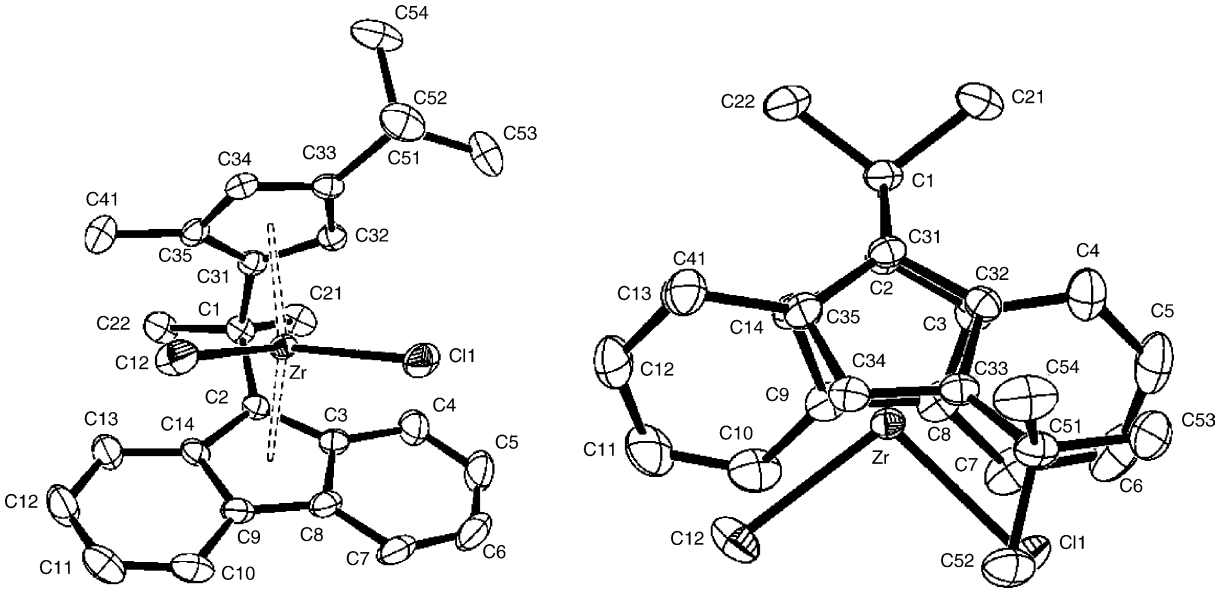

Fig. 9. Two views of the molecular structure of (η^5-3-^{t}But-5-Me-C_5H_2–CMe_2-η^5-$C_{13}H_8$)$ZrCl_2$ (**6**).

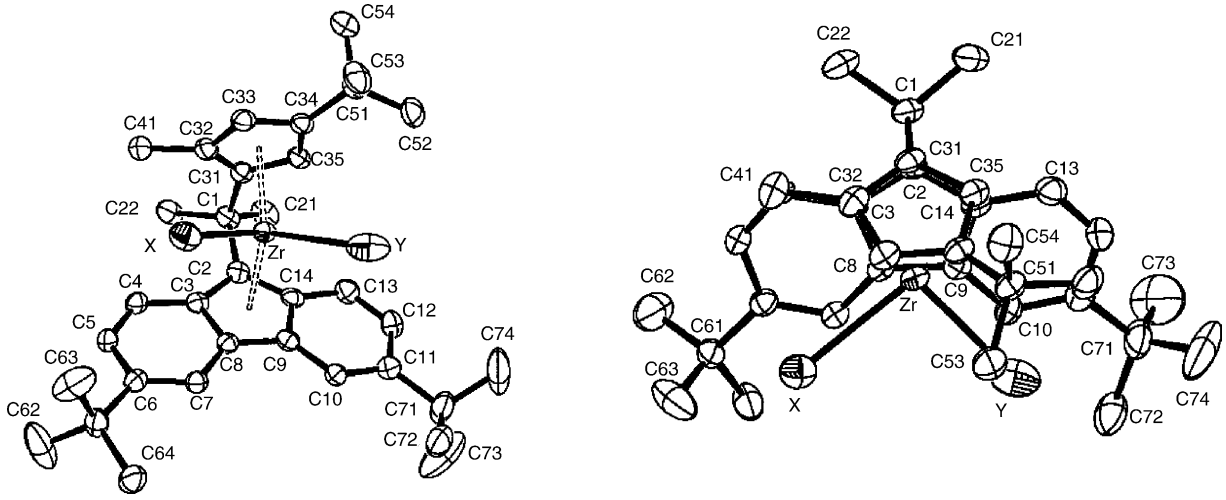

Fig. 10. Two views of the molecular structure of (η^5-3-^{t}But-5-Me-C_5H_2—CMe_2-η^5-3,6-di-^{t}But-$C_{13}H_6$)$ZrCl_2$ (**7**).

quasi-complete suppression of the regiodefects in isotactic polymers of **6** would mean that practically every monomer which is coordinated at the less crowded site in **5**, must have adopted a regio irregular coordination mode. This would further mean that any time the chain is forced to the crowded coordination position, in the absence of any other steric factors, it forces the reverse face coordinated propylene to rotate and adopt a 2-1 coordination mode and undergo a regio irregular insertion. The *trans*-proximal methyl substituent in **6**, by its non-bonded steric interaction, apparently counter balances the steric force of the polymer chain on the propylene monomer and prevents this rotation.

At this stage, we can only speculate about the true reasons for the observed regioselective behavior. It may well be related to the lateral-rotation of the transition metal active center entity within the ligand framework in the transition state [15]. By performing this rotation, the C_1 symmetric site could release some of the steric tensions that are created by the presence of different substituents, and provide more space and different positioning for the growing polymer chain and coordinating monomer (vide infra). Future, more detailed investigations of these catalyst systems and their products should shed more light on the polymerization behavior of C_1 symmetric systems and metallocene catalysts in general.

3.3. Perfect chain stationary insertion, perfect isoselectivity

While discussing the *Cs* symmetric syndiotactic selective systems we showed that the bulky substitution in the frontal position(s) 3, 6 is very beneficial for the catalyst's enantioselectivity. The frontal bulky substituent(s) not only interact(s) with the counter ions but also because of their frontal extension, interact strongly in a non-bonded fashion with the growing polymer chain and enforce its preferred orientation in the empty quadrant(s) next to the cyclopentadienyl moiety of the ligand. As a result, a tighter chiral pocket is formed in which the corresponding re and si monomer faces would fit better, thus resulting in an increase of catalyst selectivity.

The same argument should principally hold for C_1 symmetric isotactic selective catalyst systems albeit only for the less crowded coordination site. To prove this hypothesis we prepared the new metallocene molecule **7**. Fig. 10 presents the front and top views of the molecular structure of the metallocene, (η5-3-^{t}But-2-Me-C_5H_2—CMe_2-η5-3,6-di-^{t}But$C_{13}H_8$)$ZrCl_2$ (**7**) determined by single crystal X-ray diffraction methods. Table 5 summarizes the results of polymerization and the polymer properties of isotactic polypropylene formed with the **7**/MAO catalyst system at different polymerization temperatures.

As expected, the data in Table 5 indicate that the isotactic polymers produced with **7** exhibit not only higher molecular weights compared to the corresponding polymers produced with **6** but also show substantially higher stereo regularities. As demonstrated by higher mmmm pentad concentrations and melting points of the polymers. Similarly, no regiodefects have been detected for the polymers of **7**. The data in Table 5 also reveal a similar correlation between polymerization temperature and catalyst stereoselectivity as was observed with **6**, confirming the prevalence of the site epimerization process and chain "stationary" insertion mechanism for this catalyst system as well. By increasing the polymerization temperature from 40 to 60 °C, catalyst stereoselectivity is increased

Table 5
Results of polymerization and the polymer properties of isotactic polypropylene formed with the **7**/MAO catalysts system

T (°C)	M_w (kDa)	mmmm (%)	Regiodefects %	Mpt. (°C)
40	1.363	97.30	nd	157.2
60	515.4	98.07	nd	161.4
80	215.0	94.18	nd	155.7

nd, Not detected; kD, kilo Dalton.

as apparent by polymer melting points and tacticity index (mmmm %). However, when the temperature is further raised from 60 to 80 °C, the beneficial effect of the site epimerization rate increase on stereo-selectivity is overcompensated by an increasing number of reverse-face selective errors.

With **7** we have for the first time a metallocene catalyst that produces, at relatively high polymerization temperatures, isotactic polypropylene polymers with high melting point and molecular weight, matching the isotactic polymers that are commercially produced with the high performance isotactic selective Ziegler-Natta catalyst systems with the additional advantage of having very narrow molecular weight distribution.

To arrive at such a high degree of catalyst performance perfection, exhibited by **7**, the gradual improvement of our understanding of the underlying mechanistic aspects of polymerization, better resolution and interpretation of polymer analytical data, particularly ^{13}C NMR spectral data, and major advances in synthetic skills for the preparation and isolation of sophisticated metallocene pre-catalyst components were essential. Prior and parallel to the systematic application of site selective substitution both in the cyclopentadienyl and fluorenyl moieties of the bridged ligand – which we have been using as a very versatile tool to systematically modify and/or improve the different aspects of catalyst/polymerization performance – it was essential to overcome many mechanistic, analytical, and preparative challenges.

The initial ideas and models were modified based on which perfect bilateral symmetry (C_s symmetry) and homotopic coordination positions were considered as prerequisites for syndiospecificity. This allowed more dynamic models with more emphasis on polymer chain position, orientation and migration (vide infra) as more structures were discovered whose symmetry grossly diverged or simply differed from perfect C_s symmetry. For C_1 symmetric systems, the notion of the chain "stationary" insertion mechanism was introduced as a working hypothesis to explain the formation of isotactic polypropylene with **5**. This hypothesis, that did not seem obvious at the time, helped us to rationalize the polymerization behavior of the catalysts and microstructure of the resulting polymers. Subsequently, it also led to the construction of molecule **6** with much better catalytic performance. Finally, the application of these ideas developed for the C_1 symmetric system, combined with results coming from the syndiotactic system with respect to the effect of frontal substitution on the fluorenyl group, led to the development of the high performance isotactic selective catalyst **7**/MAO for which the absolute dominance of site epimerization and the perfect function of the chain "stationary" insertion mechanism is evident (cf. Fig. 10).

4. A more dynamic model

The original catalytic model applied the chain migratory insertion mechanism to the catalysts formed with the C_s symmetric metallocenes of the type depicted in Fig. 1. It was perfectly appropriate to explain the formation of syndiotactic polymers with such highly symmetric catalyst systems. According to the transition state scheme shown in Fig. 11, the catalyst's regularly alternating enantiofacial preference for the prochiral monomers that leads to the syndiotactic polymer, arises from propylene insertion taking place at regularly alternating homotopic sides at the wedge of the pseudo tetrahedral active site. However, the discovery of new syndiotactic specific structures with less than C_s perfect symmetry which produce syndiotactic polypropylene with relatively high regularities [3f,18] and structures such as **3**, with perfect C_s symmetry but no stereoselectivity, reveal that too much importance was attributed to the static features of the catalysts.

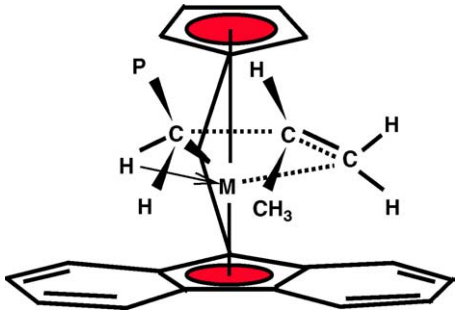

Fig. 11. Proposed transition state structure model for syndio-selective active site.

On the other hand structures such as **3** with perfect C_s symmetry but no stereoselectivity reveal that too much importance was attributed to the static features of the catalysts.

It is now evident that despite its simplicity and convenience, the original model has major handicaps. It has been conceived from images obtained from X-ray analysis performed on molecules contained in the solid-state. These rigid and static images reflect only snap shots of the fluxional, constantly vibrating, bending and "breathing" molecules. They should be considered only as frozen images and reflect only one aspect, the general shape and outline of the molecules. They do not reflect the whole "reality" of individual, freely floating molecules in the solvent medium. Additionally, any involvement with and interaction with the counter ion were ignored in most cases.

The M-centroid η^5 bonding which is shown casually in these images, is, with high probability not correct and should be rather considered as η^3 although a reversible η^5 η^3 η^1 equilibrium centered on η^3 would be an even more realistic description of the events. The basic chemistry of these compounds as well as their NMR data [2e] are indicative of their haptotropic and fluxional nature. These facts are often intentionally neglected for the sake of simplicity. However, one should be aware that dynamic phenomena are actively involved, one way or another, in different steps of the polymerization. For example, the phenomenon of hapticity change or bond order variation and ring slippage should

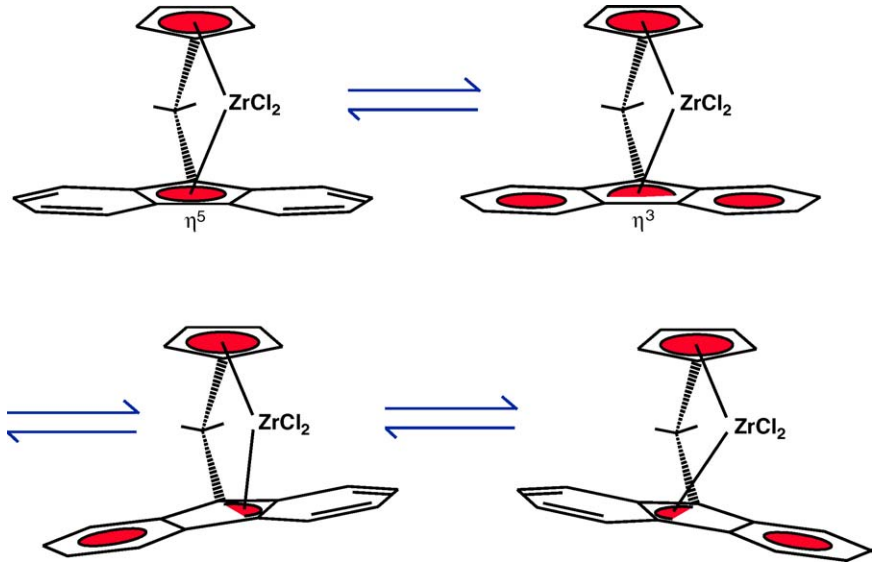

Fig. 12. Hapticity change (top) and occasional ring slippage (bottom).

be seriously considered to be involved in bridged metallocene catalysts and those involving indenyl- and fluorenyl groups as we have demonstrated [2a] (Fig. 12).

Both haptotropy and ring slippage can influence temporarily or "permanently" the electronic properties of the active site and the steric environment surrounding it and have an impact on the molecular weight and tacticity of their polymers. Another dynamic phenomenon, certainly involved in metallocene catalysis, is related to geometry change of the catalysts during the coordination and insertion steps. The pseudo tetrahedral geometry that is assumed for the tetra-coordinated transition metal in the transition state, cannot be further extended to the step just after insertion. At this stage, the tetra-coordinated structure collapses due to the disappearance of a ligand, leaving a tri-coordinated species behind in which the repulsive forces acting upon the bonding electron pairs are different and require a new geometry. The most logical structure that can be suggested for this step would be a pyramidal one (Fig. 13 right). After the next monomer coordination, the structure will again adopt the tetrahedral geometry (Fig. 13 left). This change in geometry, operating on all types of metallocene based catalyst systems, has probably more importance for the syndiospecific case where dynamic processes, such as chain migration, site epimerization (vide infra) and interaction with counter ion are vital for its existence. They also provide a clue as to why the perfect bilateral symmetry (C_s) is not so crucial for syndio-selectivity, since even the most perfect bilaterally symmetric systems will not maintain their "perfect" symmetry while acting as an active site.

Finally, another ligand/transition metal related dynamic behavior, discovered by Petersen [15] and acting on the transition state structure, is the lateral displacement of the whole ligand system around the transition metal. This movement that can be described as a kind of wind-shield wiper type oscillation of the MCl_2 moiety within the fixed ligand system can facilitate or influence the site epimerization or chain migration mechanism and may be the true reason behind unexpectedly high regioselectivties of C_1 symmetric catalyst systems (Fig. 14).

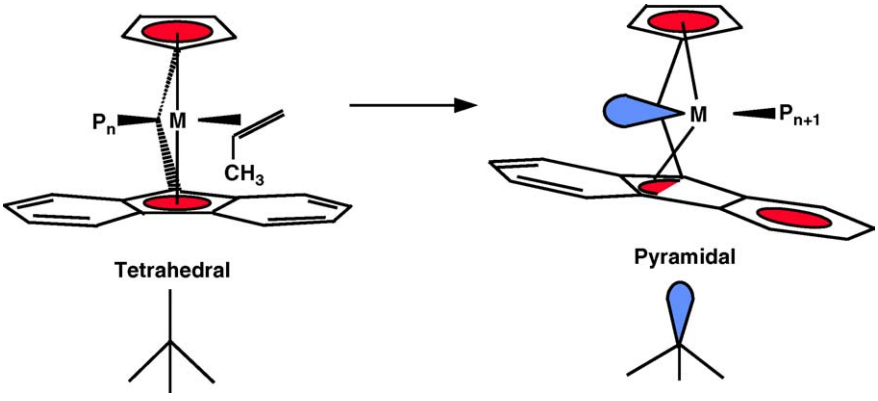

Fig. 13. Geometry variation during coordination and insertion steps.

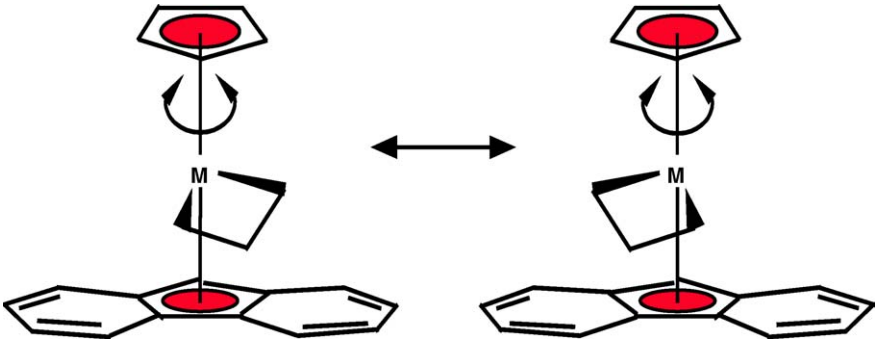

Fig. 14. Lateral displacement of the centroid-Zr bond axis (the bridge is omitted for the sake of clarity).

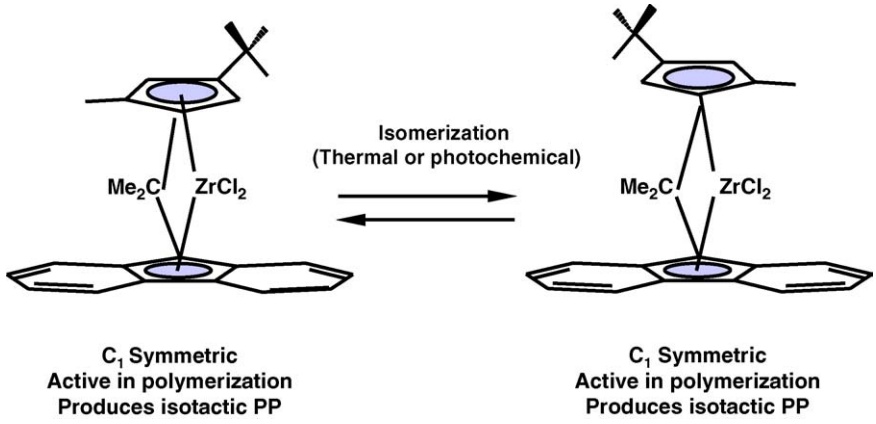

Fig. 15. Irrelevance of thermally or photochemically induced isomerization in C_1 symmetric structures for their catalytic performance.

5. C_1 symmetry versus symmetry C_2

Before ending this discussion we should emphasize some interesting and practical aspects of isotactic specific C_1 symmetric catalysts. The C_1 symmetric metallocene molecules do not undergo photo- or heat-induced isomerization during activation/heterogenization processes, nor is any meso stereoisomer formed during their synthesis (atactic fraction free isotactic polypropylene). Their stereoselectivities do not suffer by increasing the polymerization temperatures; and in some C_1 symmetric systems (vide supra) they are even boosted. The *trans* disubstituted C_1 symmetric systems are very regioselective and maintain this property upon activation/heterogenization. This is a major departure from the C_2 symmetric, bridged bis indenyl catalyst systems where not only is a meso isomer formed during the synthesis but the purified racemic forms also tend to isomerize and produce a fraction of meso isomer upon heat or light exposure. The *trans* substituted C_1 symmetric systems are very regioselective [16] and maintain this property upon activation/heterogenization.

Finally, our discussion in this paper was limited to the bridged cyclopentadienyl-fluorenyl ligand based systems and did not cover other syndiotactic specific systems which have been discussed in several recent publications [17–19]; however, the principles discussed in this paper are universally applicable (Fig. 15).

6. Experimental

6.1. Synthetic part

The synthetic procedures for the preparation of metallocene structures are more or less similar to the procedures described in Refs. [1f and k].

6.2. X-ray data

Crystallographic and molecular structure information on the new zirconium complexes with an ansa-Cp-CR_2-Flu ligand (4, 6, and 7).

The new complexes are characterized here by their space groups and lattice constants at room temperature and are as follows:

- **4**: $C_{45}H_{50}Cl_2Zr$·solvent (solvent: disordered cyclohexane); $P2_1/n$; $a = 18.448(11)$ Å, $b = 11.862(6)$ Å, $c = 21.213(10)$ Å; $\beta = 114.96(5)^\circ$.
- **6**: $C_{26}H_{28}Cl_2Zr$; P-1; $a = 8.974(1)$ Å, $b = 11.315(2)$ Å, $c = 11.627(2)$ Å; $\alpha = 85.96(2)$ Å, $\beta = 85.52(2)$ Å, $\gamma = 71.89(2)^\circ$.
- **7**: $C_{34}H_{44}ClIZr$; Pnma; $a = 12.063(2)$ Å, $b = 22.108(3)$ Å, $c = 23.568(3)$ Å. There is positional disorder at the Zr atom: each of the two halogen positions (*X* or *Y*; see Fig. 10)) can

be occupied by Cl. The other position is then occupied by *I*.

Additional details of the X-ray crystallography will be published elsewhere. Only some results concerning the molecular structure are of interest in the context of the present paper. The complexes are illustrated in Figs. 5, 9 and 10. The individual complexes **6** and **7** are chiral. Both compounds crystallize as racemates. **4** has mirror symmetry. All three complexes crystallize in centrosymmetric space groups. Structural parameters of the complexes are compared in Table 6 with those of other complexes containing a Cp-CR_2-Flu ligand, inter alia, (η^5-3-$SiMe_3$–C_5H_3–CMe_2-η^5-$C_{13}H_8$)$ZrCl_2$ (**5′**) [2a,3a]. The latter complex contains a $SiMe_3$ group at the position where **5** contains a *tert*-butyl group. The angles used and their symbols are explained in Fig. 16. The data show that the geometrical parameters for complexes with a Cp-CR_2-Flu ligand are uniform. The angle α (centroid-Zr-centroid angle) falls in the narrow interval 118.0–119.1° and β (angle between the best C_5 ring planes) falls in the interval 71–74°.

The bonding angle Φ at the bridging *C* atom is close to 99° in all complexes. The complexes show deviations from the ideal geometry, where (i) the C–C bond vector connecting the bridging C atom with the C_5 ring would be parallel to the C_5 ring plane, and (ii) a metal atom would reside exactly above the center of a C_5 ring. The deviations from this situation are measured by the angles γ and δ (see Fig. 16). δ larger than zero indicates that the metal atom is displaced from the geometrically ideal position towards the bridge. The data in Table 6 show that δ for a fluorenyl ring is considerably larger than for a C_p ring. A δ value greater than zero is accompanied by an increase of metal to ring carbon distance toward the open side of the wedge formed by the η^5 groups. The

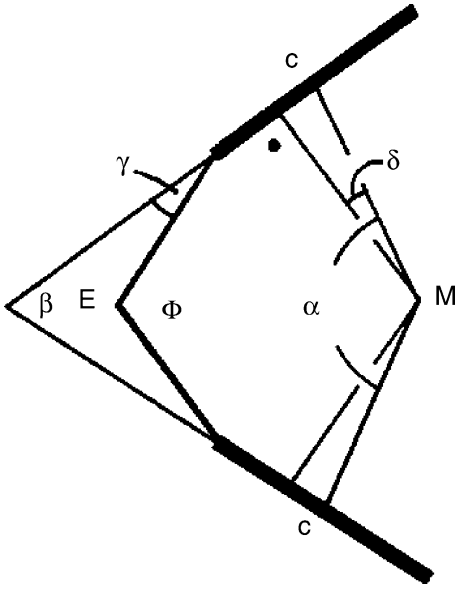

Fig. 16. Sketch indicating the angles used to describe the geometry of the bridging ligands.

Table 6
Geometrical parameters (° or Å) for zirconium complexes with a Cp-CR_2-Flu ligand

No.	Formula	ϕ	α	β	γ	δ	r (M–C_{ring}); Δr	Reference
2′	[(η^5-C_5H_4–CMe_2-η^5-$C_{13}H_8$)$ZrMe(PMe_3)$]$^+$ [$B(C_6F_5)_4$]$^-$	98.4	119.1	71.1	Cp: 15.5, Flu: 11.8	3.4, 7.1	2.43–2.55; 0.12, 2.38–2.64; 0.26	[1h]
4	(η^5-C_5H_4–CPh_2-η^5-3,6-di-′But-$C_{13}H_6$)$ZrCl_2$	99.1	118.1	73.3	Cp: 15.7, Flu: 10.2	2.8, 8.5	2.42–2.52; 0.10, 2.42–2.72; 0.30	This work
5	(η^5-3-′But-C_5H_3–CMe_2-η^5-$C_{13}H_8$)$ZrCl_2$	99.4	118.4	74.0	Cp: 13.3, Flu: 12.1	5.5, 7.3	2.43–2.62; 0.19, 2.41–2.68; 9.27	[5a]
5′	(η^5-3-$SiMe_3$–C_5H_3–CMe_2-η^5-$C_{13}H_8$)$ZrCl_2$	98.3	118.0	73.5	Cp: 13.7, Flu: 11.3	4.0, 7.5	2.43–2.55; 0.12, 2.42–2.70; 0.28	[3a]
6	(η^5-3-′But-5-Me-C_5H_2–CMe_2-η^5-$C_{13}H_8$)$ZrCl_2$	99.6	118.9	73.1	Cp: 13.9, Flu: 12.6	5.1, 7.1	2.43–2.61; 0.18, 2.43–2.69; 0.26	This work
7	(η^5-3-′But-5-Me-C_5H_2–CMe_2-η^5-3,6-di-′But-$C_{13}H_6$)$ZrCl_2$	100.2	118.5	73.1	Cp: 13.9, Flu: 13.5	5.1 6.9	2.43–2.61; 0.18, 2.43–2.69; 0.26	This work

values for δ, the Zr–C_{ring} distances and Δr, the difference between the largest and the smallest value are surprisingly similar for the Cp fragments as well as for the Flu fragments of the ansa complexes. The relatively large values of δ and Δr for the fluorenyl group can be attributed to: (i) repulsive non-bonded interactions between the chlorine (or other η^1-bonded ligands) on one side and carbon and hydrogen atoms of the fluorenyl C_6 rings on the other side, and (ii) an intrinsic preference of an η^5 ligand for an unsymmetrical arrangement of the observed type. This view is supported by the results of EHMO calculations for compounds with $C_{13}H_9^-$ and similar ligands [20]. Evidently both effects are cooperative here.

References

[1] (a) J.A. Ewen, L.R. Jones, A. Razavi, J.J. Ferrara, J. Am. Chem. Soc. 110 (1988) 6255;
(b) US Patent 5,334,677, invs.: A. Razavi, J.A. Ewen;
(c) US Patent 5,476,914, invs.: J.A. Ewen, A. Razavi;
(d) US Patent 6,184,326A, invs.: A. Razavi, J.A. Ewen;
(e) US Patent 4,892,851, invs.: A. Razavi, J.A. Ewen;
(f) A. Razavi, J.J. Ferrara, J. Organomet. Chem. 435 (1992) 299;
(g) A. Razavi, J.L. Atwood, J. Organomet. Chem. 459 (1993) 117;
(h) A. Razavi, U. Thewalt, J. Organomet. Chem. 445 (1993) 111;
(i) A. Razavi, D. Baekelmans, V. Bellia, Y. De Brauwer, K. Hortmann, M. Lambrecht, O. Miserque, L. Peters, M. Slawinsky, S. Van Belle, in: T. Sano, T. Uozumi, H. Nakatani, M. Terano (Eds.), Progress and Development of Catalytic Olefin Polymerization, Technology and Education Publishers, Tokyo, 2000, p. 176;
(j) A. Razavi, C. R. Acad. Sci. Paris., Ser. Iic, Chem. 3 (2000) 615;
(k) A. Razavi, K. Hortmann, V. Bellia, Synthetic Methods of Organometallic and Inorganic Chemistry, vol. 10, W.A. Herrman Ed. Publisher, Thieme, Stutgart, Germany, 2002, p. 185.

[2] (a) A. Razavi, V. Bellia, Y. De Brauwer, K. Hortmann, M. Lambrecht, O. Miserque, L. Peters, S. Van Belle, in: W. Kaminsky (Ed.), Metalorganic Catalysts for Synthesis and Polymerization, Springer, Berlin, 1999, p. 236;
(b) A. Razavi, V. Bellia, Y. Debrauwer, K. Hortmann, L. Peters, S. Sirole, S.V. Belle, V. Marin, M. Lopez, J. Organomet. Chem. 684 (2003) 206;
(c) A. Razavi, V. Bellia, Y. Debrauwer, K. Hortmann, L. Peters, S. Sirole, S.V. Belle, Macromol. Sym. 213 (2004) 157;
(d) H.G. Alt, M. Jung, G. Kehr, J. Organomet. Chem. 562 (1998) 153;
(e) D. Drago, P.S. Pergosin, A. Razavi, Organometallics 19 (2000) 1802;
(f) A.K. Dash, A. Razavi, A. Mortreux, C. Lehmannand, J.F. Carpentier, Organometallics 21 (2002) 3238;
(g) E. Kirilov, L. Toupet, C.W. Lehmann, A. Razavi, S. Kahlal, J.Y. Saillard, J.F. Carpentier, Organometallics 22 (2003) 4038;
(h) E. Kirilov, L. Toupet, C. Lehmann, A. Razavi, J.F. Carpentier, Organometallics 22 (2003) 4467;
(i) E. Kirilov, C. Lehmann, A. Razavi, J.F. Carpentier, Eur. J. Inorg. Chem. (2004) 943;
(j) E. Kirilov, C. Lehmann, A. Razavi, J.F. Carpentier, Organometallics 23 (2004) 2768;
(k) E. Kirilov, C. Lehmann, A. Razavi, J.F. Carpentier, J. Am. Chem. Soc. 126 (2004) 12240;
(l) A. Razavi, V. Bellia, Y. Debrauwer, K. Hortmann, L. Peters, S. Sirole, S.V. Belle, U. Thewalt, Macromol. Chem. Phys. 205 (2004) 347.

[3] (a) A. Razavi, U. Thewalt, J. Organomet. Chem. 621 (2001) 267;
(b) EP 96111127.5, inv.: A. Razavi;
(c) Int. Patent WO 98/02469, inv.: A. Razavi;
(d) EP A1, 083188, inv.: A. Razavi;
(e) WO 00/49029 and EP-A1, 169, 356, inv.: A. Razavi;
(f) H.G. Alt, R. Zenk, W. Milius, J. Organomet. Chem. 514 (1996) 257.

[4] A. Razavi, L. Peters, L. Nafpliotis, D. Vereecke, K. Den Daw, Makromol. Sym. 89 (1995) 345.

[5] (a) A. Razavi, J.L. Atwood, J. Organomet. Chem. 520 (1996) 115;
(b) A. Razavi, L. Peters, L. Nafpliotis, J. Mol. Catal. A 115 (1997) 129.

[6] (a) A. Razavi, D. Vereecke, L. Peters, K. Den Daw, L. Nafpliotis, J.L. Atwood, in: G. Fink, R. Muelhaupt, H.H. Brintzinger (Eds.), Ziegler Catalysts, Springer-Verlag, Berlin, 1993;
(b) V. Busico, R. Cipullo, G. Talarico, Macromolecules 30 (1997) 4787;
(c) R. Kleinschmidt, M. Reffke, G. Fink, Macromol, Rapid Commun. 20 (1999) 284;
(d) A. Razavi, C. R. Acad. Sci. Paris, Ser. IIc, Chem./Chem. 3 (2000) 615.

[7] (a) L. Cavallo, G. Guerra, M. Vacatello, P. Corradini, Macromolecules 24 (1991) 1784;
(b) G. Guerra, L. Cavallo, L. Moscardi, M. Vacatello, P. Corradini, Macromolecules 29 (1996) 8434.

[8] (a) W.E. Piers, J.E. Bercaw, J. Am. Chem. Soc. 112 (1990) 9406;
(b) H.H. Brintzinger, H. Krauledat, Angew. Chem. Int. Ed. Engl. 29 (1990) 1412;
(c) H.H. Brintzinger, M.L. Leclerc, J. Am. Chem. Soc. 117 (1995) 1651;
(d) B.J. Burger, W.D. Cotter, E.B. Coughlin, S.T. Chascon, S. Hajela, T.A. Herzog, R.O. Koehn, J.P. Mitchell, W.E. Piers, P.J. Shapiro, J.E. Bercaw, in: G. Fink, R.H. Muelhaupt, H.H. Brintzinger (Eds.), Ziegler Catalysts, Springer-Verlag, Berlin, 1995;
(e) R.H. Grubbs, G.W. Goates, Acc. Chem. Res. 29 (1996) 85.

[9] Other examples of aspecific catalysts with C_s symmetric metallocene are the complexes iPr(3,4-dimethylcyclopentadienyl-fluorenyl)-ZrCl2 and dimethylsilyl(cyclypentadienyl-tetramathylcyclopentadienyl)ZrCl2 see also [1j and 19a].

[10] Bulky substitution in proximal position(s) of 1 could bring about some improvement in stereoregularity yet the synthesis of these compounds should not be easy.

[11] (a) E.Y.-X. Chen, T.J. Marks, Chem. Rev. 100 (2000) 1391;
(b) B. Rieger, C. Troll, Macromolecules 35 (2002) 5742;
(c) V. Busico, R. Cipullo, F. Cutillo, M. Vacatello, V.A. Castelli, Macromolecules 36 (2003) 4258;
(d) N. Herfert, G. Fink, Macromol. Symp. Rapid Commun. 66 (1993) 157;
(e) N. Herfert, G. Fink, Makromol. Chem. 193 (1992) 773.

[12] (a) P. Cossee, J. Catal. 3 (1964) 99;
(b) E.J. Arlman, J. Catal. 3 (1964) 89;
(c) E.J. Arlman, P. Cossee, J. Catal. 3 (1964) 99.

[13] (a) H.H. Brintzinger, D. Fischer, R. Muelhaupt, R.B. Rieger, R.M. Waymouth, Angew. Chem. Int. Ed. Engl. 20 (1995) 1143;
(b) L. Resconi, L. Cavallo, A. Fait, F. Piemontesi, Chem. Rev. 100 (2000) 1253.

[14] (a) EP-A-1, 155050, inv.: A. Razavi;
(b) WO 98/54230, inv.: A. Razavi, US Patent 6,265,505, inv.: Razavi;
(c) WO 98/54230, inv.: A. Razavi.;
(d) WO 00/49029, inv.: A. Razavi, V. Bellia.

[15] A. Kabi-satpathy, C.S. Bajgur, K.P. Reddy, J.L. Petersen, J. Organomet. Chem. 364 (1989) 105.

[16] (a) G. Guerra, P. Longo, L. Cavallo, P. Corradini, L. Resconi, J. Am. Chem. Soc. 119 (1997) 4394;
(b) G. Guerra, L. Cavallo, G. Moscadi, G. Vacatello, P. Corradini, J. Am. Chem. Soc. 116 (1994) 2988;
(c) M. Toto, L. Cavallo, P. Corradini, G. Moscardi, L. Resconi, G. Guerra, Macromolecules 31 (1998) 3431.

[17] (a) T.A. Herztog, L. Zubris, J.E. Bercaw, J. Am. Chem. Soc. 118 (1996) 11988;
(b) D. Veghini, J.E. Bercaw, Polym. Reprints 39 (1) (1998) 210;
(c) S.A. Miller, J.E. Bercaw, Organometallics 21 (2002) 934.
[18] (a) R. Leino, F.J. Gomez, A.P. Cole, R.M. Waymouth, Macromolecules 34 (20012082);
(b) F.J. Gomez, R.M. Waymouth, Macromolecules 35 (2002) 358.
[19] (a) A. Zambelli, I. Sessa, F. Grisi, R. Fusco, P. Accomazzi, Macromol. Rapid Commun. 22 (2001) 297;
(b) C. Pellecchia, A. Zambelli, M. Mazzeo, D. Pappalardo, J. Mol. Catal. A: Chem. 128 (1988) 229;
(c) J. Tian, G.W. Coates, Angew. Chem. Int. Ed. 39 (2000) 3626;
(d) J. Tian, P.D. Hustad, G.W. Coates, J. Am. Chem. Soc. 123 (2001) 5134;
(e) J. Saito, M. Mitani, J. Mohri, S. Ishii, Y. Yoshida, T. Matsugi, S. Kojoh, N. Kashiwa, T. Fujita, Chem. Lett. (2001) 567;
(f) J. Saito, M. Mitani, J. Mohri, S. Ishii, Y. Yoshida, T. Matsugi, S. Kojoh, N. Kashiwa, T. Fujita, J. Am. Chem. Soc. 124 (2002) 7888.
[20] A. Decken, J.F. Britten, M.J. Mc Glinchey, J. Am. Chem. Soc. 115 (1993) 7275.